Article

Modeling and Simulation of Reel Motion in a Foxtail Millet Combine Harvester

Zhenwei Liang *, Jia Liu, Deyong Yang and Kangcheng Ouyang

School of Agricultural Engineering, Jiangsu University, Zhenjiang 212013, China;
2222316025@stmail.ujs.edu.cn (J.L.); yangdy@ujs.edu.cn (D.Y.); 3230306046@stmail.ujs.edu.cn (K.O.)
* Correspondence: zhenwei_liang@ujs.edu.cn

Abstract: Due to the high plant height, heavy ear, and easy forward tilt of millet during harvesting, the reel of a traditional combine harvester is often difficult to adapt to the special growth characteristics of millet, resulting in serious grain loss. Therefore, optimizing the design of the reel is important to improve the harvesting efficiency of millet and reduce the grain header loss. In order to determine the optimal reel speed ratio(λ), kinematics simulation experiments and analysis were carried out under different combinations of forward speed and reel revolution speed. The results showed that the supporting effect of the reel is insufficient when $\lambda \leq 1$, and the trochoidal trajectory of the reel can provide a backward driving force when $\lambda > 1$, the optimum speed ratio of the reel should be controlled between 1.5 and 1.6. Field experiments results showed that the grain header loss rate was the lowest (0.9%) when $\lambda = 1.6$. This study provides key guidance for the adjustment of the combine harvester, effectively reducing the grain header loss rate in harvesting millet, and improving the harvesting efficiency.

Keywords: foxtail millet; combine harvester; reel; reel speed ratio; RecurDyn

1. Introduction

Millet is one of China's primary minor grain crops, with a cultivation area of approximately 2 million hectares. It is highly nutritious, rich in protein, fats, and vitamins, serving both as a food crop and as high-quality animal feed, thus providing both dietary and economic value [1]. While rice, wheat, and rapeseed benefit from continuous advancements by scholars in threshing efficiency, cleaning performance, and noise reduction [2–8], the low mechanization rate in millet harvesting remains a major constraint to expand millet cultivation further. In recent years, to enhance the mechanized harvesting of millet, numerous researchers and manufacturers have modified rice and wheat combine harvesters to meet the specific requirements for millet harvesting.

Hobson et al. conducted a comparative study on two different cutting platforms to reduce the cutting platform loss rate in combine harvesters. Their findings revealed that the loss rate of a header equipped with an additional conveyor device behind the main cutter was half that of a standard cutting platform [9]. Hirai et al. explored the interaction between the combine harvester reel and crop stems, determining that the mass of the harvested crop ears is directly proportional to the force exerted by the reel [10]. Wu et al. studied header loss in rapeseed combine harvesters. By analyzing the effects of the reel's horizontal position, vertical position, and rotational speed on loss rate and feed rate, they found that reel revolution speed had the most significant impact on feed rate. The optimal parameter combination for the header was identified as a reel horizontal position of 50 mm, a vertical

position of 1056 mm, and a rotational speed of 30 rpm, resulting in a grain header loss rate of 1.01% and a feed rate of 8.48 kg/s [11]. To address header blockage in green forage corn harvesters, Zhao constructed a test bench and analyzed the influence of forward speed, cutting height, and number of rows on specific energy consumption and grain header loss. He proposed a combined response surface method (RSM)–artificial neural network (ANN) approach to model and predict the header's performance parameters. The optimal combination was found to be a forward speed of 1.6 km/h, a cutting table height of 167 mm, and four cutting table rows [12]. Zhao et al. developed the 4LZG-1.5 small, self-propelled millet harvester, designed for hilly and mountainous regions, as well as small plots in plains. The design includes a millet-specific crop lifter and an extended contour-following header, utilizing a composite threshing rotor ("rib-bar + board-tooth + spike-tooth") and a small-hole mesh sieve separation mechanism. After improvements, the total grain loss rate was reduced to 4.5%, with an impurity rate of 2.2% and a breakage rate of 3.1% [13]. Zheng et al. used ANSYS software R18.1 to conduct finite element analysis on the cutting platform frame, optimizing weak structural areas in the millet header design. This ensured that the natural frequencies of the header frame avoided the excitation frequencies of external forces, reducing the loss rate by 14.5% [14]. Yang et al. simulate the reel's motion trajectory through both mathematical and physical models. Seven different methods were used to model the reel's movement, revealing its motion dynamics [15]. Li et al. focused on reducing resonance in combine harvester operation by adjusting the structure of the header frame. By reducing the thickness of the crossbeam and curved beam by 0.2 mm, and the thickness of the base plate and side plates by 0.4 mm, the mass of the platform frame was reduced by 14.02%. Additionally, increasing the balance weight of the drive shaft by 254.90 g effectively prevented resonance [16]. To meet the demands of multi-crop harvesting and reduce harvesting losses, Ji et al. designed methods to adjust the rotation and forward speeds of the reel. Their experiments showed that the best harvesting results and lowest loss rate occurred when the reel speed ratio (λ) was between 1.4 and 1.8 [17]. Li et al. studied the principles of crop division during millet harvesting and designed a crop divider specifically suited for millet. The structural design of the divider was validated through virtual simulation technology, confirming its effectiveness [18]. Du et al. designed an automatic control device for the reel's rotational speed in a rice-wheat combine harvester, allowing it to operate at a stable and appropriate speed. Experimental tests showed that when the reel speed ratio was set to 1.3 and the working speed varied between 4 and 7 km/h, the maximum relative error in reel speed adjustment was 8.6%, with accuracy exceeding 90% [19]. While these research results provide valuable theoretical and practical guidance for optimizing harvesters for conventional crops like rice, wheat, and rapeseed, most studies focus on these crops. There is relatively little research on the design and optimization of harvesting equipment for crops like millet, which have high stalks and complex ear structures. The natural growth height of millet generally ranges from 1100 mm to 1500 mm, whereas the typical harvest height for rice and wheat is between 700 mm and 1100 mm. Therefore, when millet is harvested using a rice-wheat combine harvester, the millet stems cut by the header may slide off the header together with the ear due to insufficient header depth. Furthermore, the ear layer of mature millet can vary significantly, depending on the bending degree of the plant and the drooping range of the ear head. This makes traditional grain joint harvesting methods ineffective due to improper reel positioning.

The reel is a crucial working element of the combine harvester's header and it is the first component to engage with the crop. Its primary function is to lift and guide the crop upright into the header, enabling the cutter to cut the crops efficiently [20]. Studies have shown that modified millet combine harvesters often face challenges such as feeding

difficulties and high total grain loss rates, with header losses accounting for approximately 40% of the total loss [21–23]. The ratio of the reel's rotational speed to the harvester's forward speed varies with different harvesting conditions, making precise control of the reel's motion trajectory essential for optimizing harvesting efficiency.

The analysis highlights that traditional grain combine harvesters are ineffective for harvesting mature millet. As a tall crop with large, heavy, and elongated ears, mature millet exhibits significant variation in panicle layers due to differing stem bending and panicle droop. In conventional grain harvesters, improper reel positioning often leads to suboptimal crop handling. Therefore, this study focuses on the reel, the first component to interact with the crop. A mathematical model was developed, and kinematic simulation analysis was conducted using virtual prototyping technology, providing a theoretical foundation for reducing crop loss during harvesting.

2. Materials and Methods

2.1. Determination of Reel Model Parameters

Structurally, reels can be classified into two types. The first is the conventional reel, which features a simple design but has limited adaptability to different crops, resulting in suboptimal harvesting performance. As a result, this type is gradually being phased out [24]. The second type, shown in Figure 1, is the eccentric reel, which is widely used in modern combine harvesters. The design parameters of the eccentric reel include the reel diameter, main shaft diameter, rotational speed, and tube shaft diameter. Additionally, the installation position of the reel must be carefully considered during assembly.
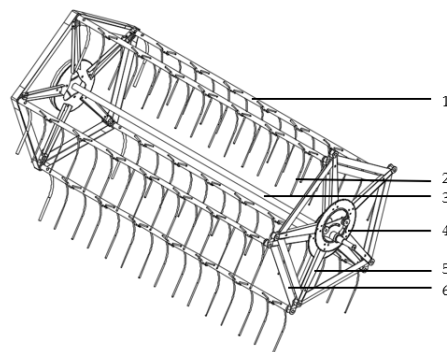
Figure 1. Structural diagram of eccentric reel. 1. Spring-tooth shaft. 2. Spring-finger. 3. Reel wheel shaft. 4. Eccentric strap. 5. Eccentric main spoke disc. 6. Main spoke disk.

2.1.1. Determination of the Number of Reel Finger Bars

The number of reel finger bars in a combine harvester varies depending on the growth conditions and yield of the harvested crop. For crops with high ear density, high yield per unit area, and grains that are not prone to shedding after maturity, the number of reel bars can be increased to enhance harvesting efficiency. Conversely, for crops that tend to shed grains easily after maturity and have a lower yield, the number of reel bars should be reduced to minimize the reel's impact on the crop during harvesting [25]. According to the Agricultural Machinery Design Handbook, the number of finger bars should be selected to ensure that an appropriate amount of crop is guided towards the cutter at a stable machine operating speed, with the recommended range typically being between 4 and 6 [26]. Given the high ear density of foxtail millet, a 5-bar reel design was chosen to minimize the crop pressure per finger bar and reduce the reel's impact on the millet.

2.1.2. Determination of Reel Diameter and Rotational Speed

The reel's rotational speed V_m can be determined using Equation (1), assuming a given operating speed n of the combine harvester.

$$n = \frac{30\lambda V_m}{\pi R} \tag{1}$$

where λ is the reel speed ratio (dimensionless), V_m is the operational speed of the combine harvester (m s^{-1}), and R is the reel radius (mm).

Based on empirical harvesting data, it has been observed that for crops like foxtail millet, which are prone to grain loss, the reel speed ratio (λ) should not be excessively high. Extensive experimentation has shown that the optimal reel speed ratio for foxtail millet lies in the range of 1.3 to 1.6. To minimize the manufacturing and maintenance costs of the combine harvester header, the reel radius is standardized to commonly used models, with a value of 450 mm. Given the rated working speed of the combine harvester (V_m = 1.2 m s^{-1}), the reel rotational speed is calculated to fall within the range of 33 to 40 rpm, as determined by Equation (1).

2.1.3. Determination of Reel Installation Height

During the operation of the combine harvester, the reel needs to exert a stable backward pushing force on the cut foxtail millet stems until the crops are tangential to the circumferential path of the header auger [27]. Therefore, the installation height (H) of the reel must satisfy the condition specified in Equation (2).

$$H = R + \frac{2}{3}(L - h) \tag{2}$$

According to Equation (2), the vertical height (H) between the center axis of the reel and the transverse cutter is calculated to be 1130 mm. However, since the height of foxtail millet crops can vary significantly across different regions, and even within the same region, research on the morphological characteristics of millet plants shows that the difference between the maximum and minimum stem heights is approximately 210 mm. With the cutting height fixed at 200 mm, the reel design should include a hydraulic adjustment mechanism that allows for a range of about 300 mm to accommodate height variations.

2.1.4. Design of the Rear Retracting Mechanism for the Reel

Compared to wheat and rice, foxtail millet has a significantly larger ear mass relative to the entire plant after maturity, which causes the crops to lean forward. In some cases, the horizontal distance from the ear head to the base of the plant can be as small as 200 mm. In contrast, the ears of wheat and rice typically grow vertically, minimizing excessive tilting. Therefore, optimizing the horizontal installation position of the reel is crucial to reduce grain loss due to impact and friction during operation. Even when grain loss occurs, the grains should ideally fall onto the header. The conventional design of combine harvesters for rice and wheat, illustrating the typical reel installation position on the header, is shown in Figure 2.

In Figure 2, H represents the installation height of the reel, B_1 denotes the forward extension length from the center axis of the reel to the cutter, and h indicates the stubble height. The forward extension amount B_1 of the combine harvester's reel can be determined using Equation (3).

$$B_{1max} = \frac{D}{2\lambda} \times \sqrt{\lambda^2 - 1} \tag{3}$$

where B_{1max} is the maximum forward extension length of the header (mm), and D is the diameter of the reel (mm).
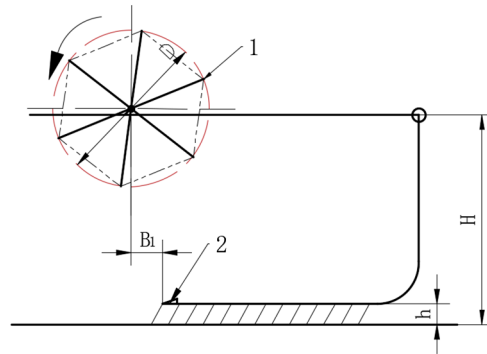
Figure 2. Schematic diagram of reel installation position in combine harvester. 1. Reel. 2. Cutter.

When harvesting rice and wheat, the diameter of the reel is typically around 900 mm, with a reel speed ratio set at 1.7. According to Equation (3), the maximum forward extension of the reel is calculated to be 363 mm. In the actual design process, while the forward extension of the reel can be adjusted depending on the type of crop being harvested, as shown in Figure 2, the traditional reel installation consistently places it in front of the cutter on the header. This positioning can cause the foxtail millet stems to be struck by the reel before entering the header, leading to grain loss outside the header. Therefore, given the tendency of foxtail millet plants to lean forward due to the weight of the ear heads after maturity, it is necessary to modify the reel's forward extension to a rear retraction. Specifically, the center axis of the reel should be positioned behind the header cutter. The improved installation schematic of the reel is shown in Figure 3.
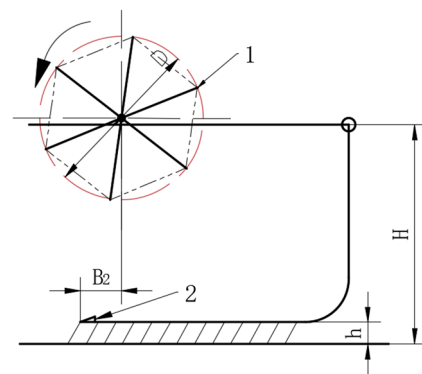
Figure 3. Schematic diagram of reel installation position of millet combine harvester. 1. Reel. 2. Cutter.

By retracting the center axis position of the reel behind the cutter on the header, the foxtail millet combine harvester can significantly reduce grain loss caused by the reel's impact during the harvesting process. Compared to a forward-positioned reel, a rear-positioned reel more effectively addresses the issue of the entire plant leaning forward due to the weight of the mature ear heads. The amount of rear retraction, denoted as B_2, should satisfy the following condition:

$$0 \leq B_2 \leq \frac{D}{2\lambda} \times \sqrt{\lambda^2 - 1} \tag{4}$$

In Equation (4), the range of the reel speed ratio (λ) is between 1.3 and 1.6, and the diameter of the reel (D) is 900 mm. Therefore, the rear retraction amount B_2 should not exceed 292 mm. Theoretically, a larger rear retraction amount facilitates grain falling into the

header; however, excessive rear retraction can hinder the reel from effectively supporting the foxtail millet stems that have been cut by the transverse cutter. Experimental results indicate that an optimal rear retraction amount of approximately 260 mm provides the best operational performance for the foxtail millet combine harvester.

2.2. Motion Model of the Reel Based on SolidWorks and RecurDyn

2.2.1. Establishment of the 3D Model of the Reel

The eccentric reel of the combine harvester primarily consists of components such as finger bars, finger bar shafts, drive shafts, and eccentric discs. The radius of the reel is determined to be 450 mm, while the standard radius of the finger bar shaft is set at 30 mm, with a length of 1800 mm. The finger bar shaft is uniformly distributed with 18 finger bars. The main shaft of the reel has a length of 2100 mm and a radius of 40 mm. Using these data, 3D modeling and assembly of each component were conducted in SolidWorks R2021 (Dassault Systemes, Pairs, France) software.

2.2.2. Establishment of the Virtual Prototype of the Reel

The 3D model of the reel created in SolidWorks was imported into RecurDyn 2023 (FunctionBay, Seongnam-si, Gyeonggi-do, Republic of Korea) software for kinematic simulation analysis to evaluate the feasibility of the designed reel structure [28,29]. To reduce the workload in subsequent simulation processes, all bolts, bearings, and various connectors and constraints within the reel were removed, allowing each component of the reel to function as independent parts.

The components of the reel's 3D model imported into RecurDyn software are initially independent of one another. To establish the necessary assembly relationships, corresponding constraints and joints must be added between the parts. To minimize the number of constraints and joints, and thus reduce the workload during simulation analysis, non-relatively moving components within the reel were merged into a single entity. Constraints and joints were then applied only to the components exhibiting relative motion. Specifically, the reel arm and fingers were merged into a single entity, and a rotational joint was added between them and the main disc [30,31]. The two main discs and the main spokes were also merged into one entity, with a rotational joint added between them and the drive shaft. Similarly, the eccentric disc and spokes were merged into a single entity, with a rotational joint established between them and the main disc. The drive shaft was treated as a single entity, with a translational joint added between it and the ground. Figure 4 shows the 3D model of the reel after the constraints were applied, with different colors representing the various constrained bodies for easy observation.
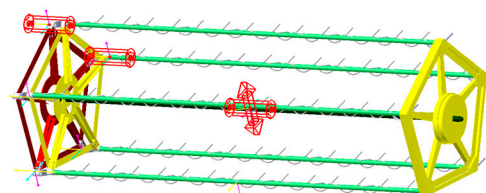
Figure 4. Reel 3D model with constraints added in RecurDyn software.

After establishing constraints and joints between the components of the reel, the next step is to access the dynamics simulation settings page. In the dynamics analysis section of RecurDyn software, the simulation time is set to 30 s, with a total of 300 simulation steps. Subsequently, the post-processing interface is used to extract the acceleration and displacement curves for the ends of the finger bars on the reel.

3. Results and Discussion

3.1. Analysis of Kinematic Simulation Test Results

3.1.1. Motion Trajectory of the Reel When $\lambda < 1$

When the reel speed ratio $\lambda < 1$, with a reel linear speed of 0.5 m s^{-1} and a combine harvester operational speed of 1.2 m s^{-1}, this results in $\lambda = 0.83$. The motion trajectory of the reel is illustrated in Figure 5.

(a)

(b)   (c)
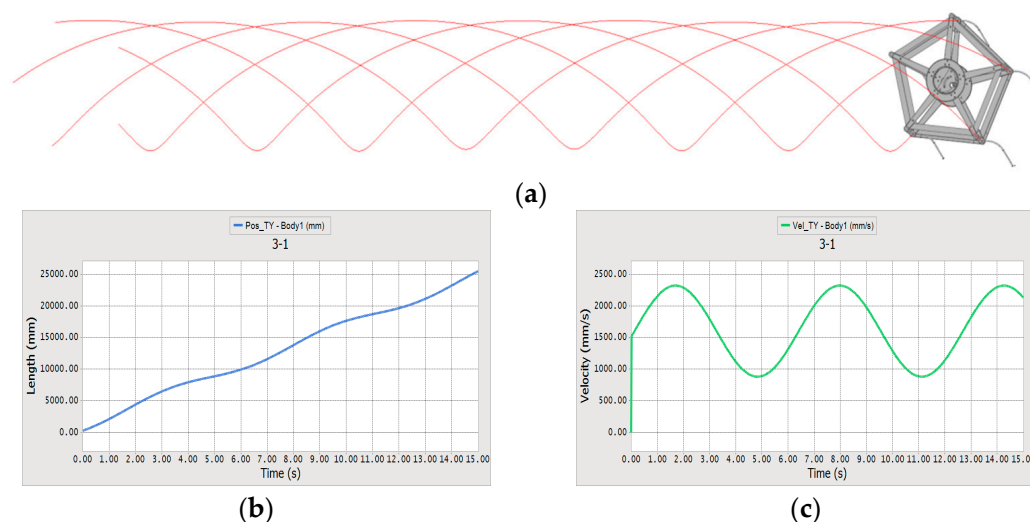
Figure 5. Reel movement status with $\lambda < 1$. (**a**) Motion trajectory of the reel arm; (**b**) Horizontal displacement curve of the finger bar ends; (**c**) Horizontal velocity curve of the finger bar ends.

From Figure 5, it can be deduced that when the reel speed ratio $\lambda < 1$, the motion trajectory of any given point on the reel arm exhibits a short-length cycloidal pattern. This pattern lacks any looping behavior, which means there is no backward pushing effect exerted on the foxtail millet plants. In this scenario, the horizontal displacement curve corresponding to the ends of the finger bar displays a slight variation. Additionally, the horizontal velocity at the ends of the finger bar consistently remains non-negative, further confirming the absence of any backward horizontal velocity. Consequently, the reel does not perform its intended functions effectively, which include supporting the crops that have been severed by the cutter and guiding them into the header.

3.1.2. Motion Trajectory of the Reel When $\lambda = 1$

When the reel speed ratio $\lambda = 1$, with the reel linear speed set at 1.2 m s^{-1} and the operational speed of the combine harvester also at 1.2 m s^{-1}, λ equals 1. The motion trajectory of the reel is depicted in Figure 6.

From Figure 6, it can be concluded that when the reel speed ratio $\lambda = 1$, the motion trajectory of the reel arm takes the form of a standard cycloidal pattern. This pattern is characterized by the absence of loops, which ensures that no backward pushing effect is exerted on the foxtail millet plants. Under these conditions, the horizontal displacement curve of the finger bar ends exhibits a slight fluctuation, and the horizontal velocity at these ends consistently remains non-negative. At no point along the trajectory is there any evidence of backward horizontal velocity, highlighting that the backward support effect provided to the harvested crops is extremely limited.

(a)

(b)

(c)
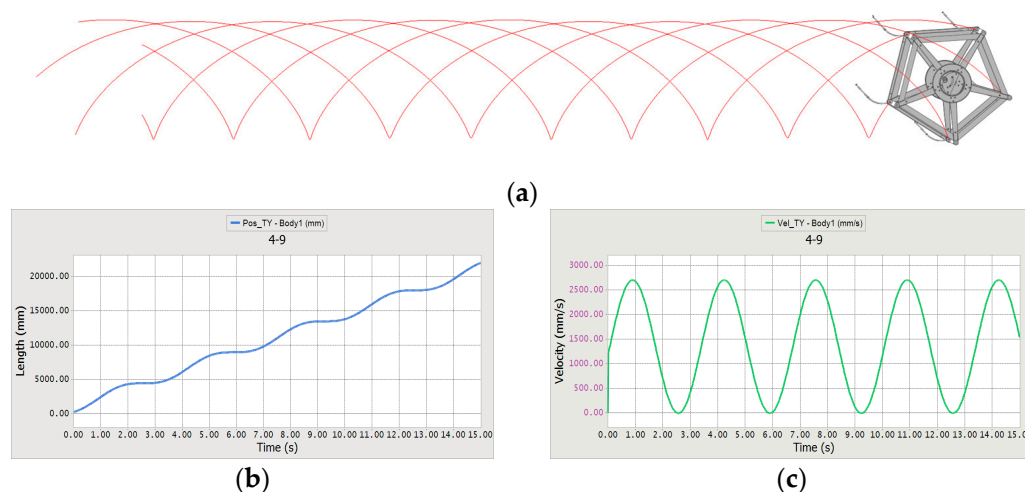
Figure 6. Reel movement status with $\lambda = 1$. (**a**) Motion trajectory of the reel arm; (**b**) Horizontal displacement curve of the finger bar ends; (**c**) Horizontal velocity curve of the finger bar ends.

3.1.3. Motion Trajectory of the Reel When $\lambda > 1$

When the reel speed ratio $\lambda > 1$, with a reel linear speed of 1.8 m s^{-1} and an operational speed of the machine set at 1.2 m s^{-1}, λ equals 1.5. The motion trajectory of the reel is illustrated in Figure 7.

(a)

(b)

(c)
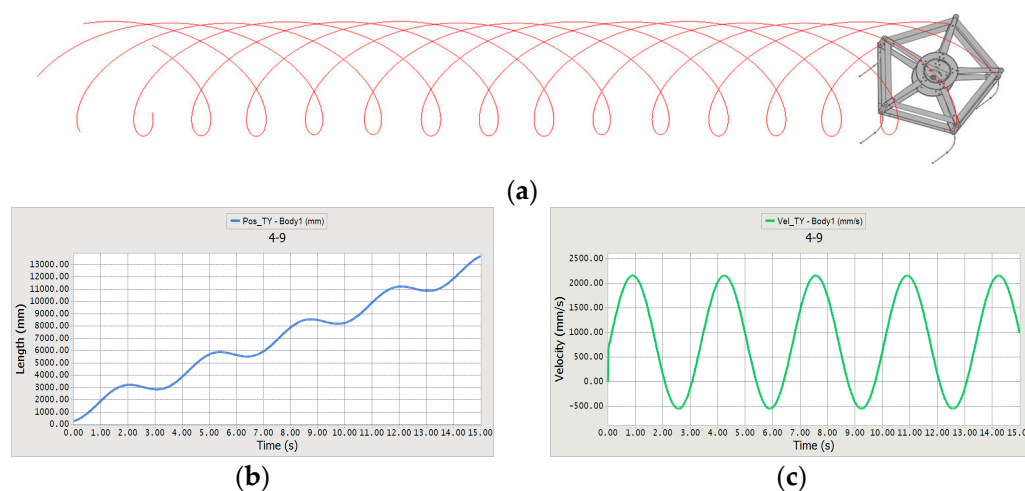
Figure 7. Reel movement status with $\lambda > 1$. (**a**) Motion trajectory of the reel arm; (**b**) Horizontal displacement curve of the finger bar ends; (**c**) Horizontal velocity curve of the finger bar ends.

From Figure 7, it can be concluded that when the reel speed ratio $\lambda > 1$, the motion trajectory of the reel arm follows a hypotrochoid pattern. This trajectory is characterized by loops, which generate a backward pushing effect on the foxtail millet crops. In this scenario, the horizontal displacement curve of the finger bar ends demonstrates significant fluctuations, reflecting the dynamic changes in the position of the finger bar. Furthermore, the horizontal velocity of the finger bar ends includes negative values, indicating that, at certain points along the trajectory, there is a backward horizontal velocity. This backward velocity allows the reel to effectively push the crops that have been severed by the cutter in a backward direction, aiding in their movement away from the cutting area and push the cut crop into the header.

3.2. Determination of the Optimal Reel Speed Ratio

From the analysis in the previous section, it can be concluded that the speed ratio (λ) had a significant effect on the header loss rate of the millet combine harvester. The simulation analysis shows that when λ > 1, the trochoidal trajectory of the reel can provide a backward driving force, effectively guiding the cut millet stem into the cutting table, and significantly reducing the loss rate. When λ ≤ 1, due to the lack of backward speed, the supporting effect of the reel is insufficient, resulting in an increase in the grain header loss rate. However, to further minimize the header losses of the combine harvester during the foxtail millet harvesting process, it is essential to identify the optimal speed ratio for millet effective harvesting. The ends of the finger bars of the reel are selected as observation points to analyze their velocity variation curves at different reel speed ratios. The results of this analysis are presented in Figures 8 and 9.
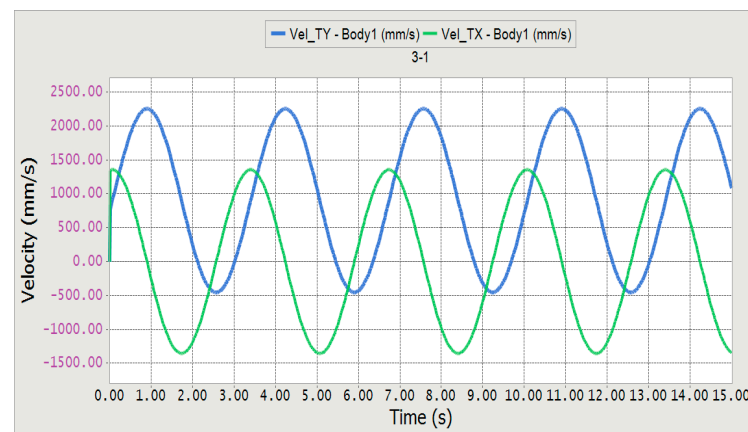
Figure 8. Reel revolution speed change curve with λ = 1.2.
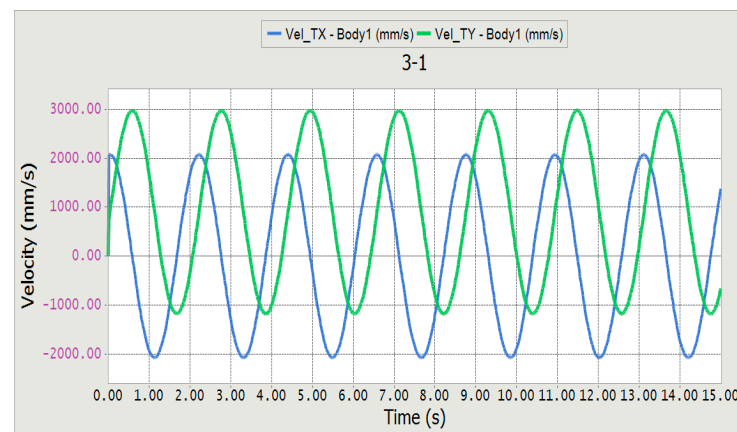
Figure 9. Reel speed change curve with λ = 1.8.

From the comparative curves of reel speed at different speed ratios, as illustrated in Figures 8 and 9, it can be observed that when the operational speed of the combine harvester remains constant, an increase in the rotational speed of the reel leads to a more pronounced amplitude of speed variation. This increase also results in a shorter motion period for the reel. While a higher rotational speed of the reel extends its effective range of operation, enabling it to engage with more of the crop, it also intensifies the impact exerted on the foxtail millet heads. This increased impact contributes to higher header losses, as more crop heads are likely to be dislodged or damaged during the harvesting process. To explore the relationship between the reel's effectiveness and the speed ratio λ, simulation results from the virtual prototype model of the reel were used to evaluate

its performance under various operating conditions [32,33]. As shown in Figure 10, when the cutter position is beneath the trajectory of the reel's action, Δx represents the effective range within which the reel supports and pushes the crop straws in a single instance.
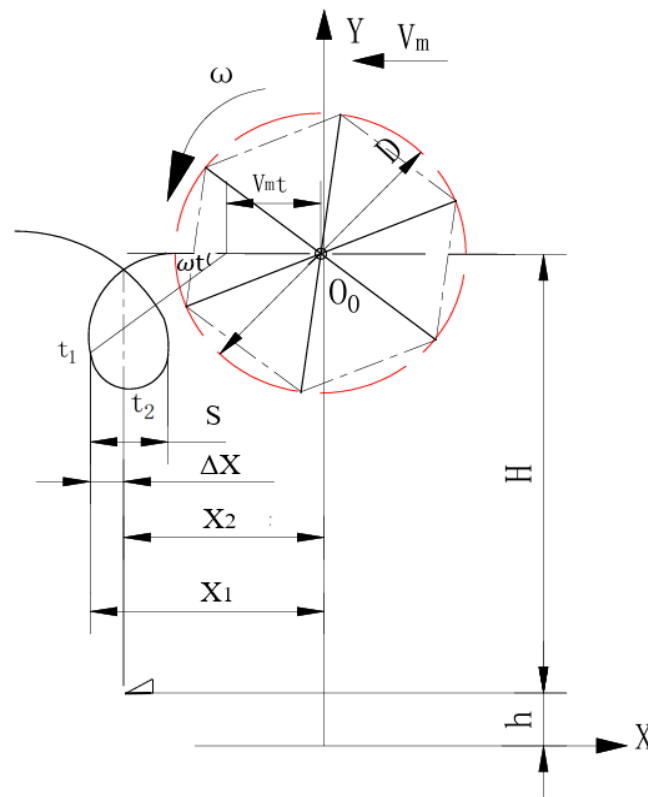
Figure 10. Schematic diagram of reel when harvesting.

Based on the geometric relationships of the reel's motion trajectory shown in Figure 10, the following equations can be established:

$$x_1 = V_m t_1 + \frac{R}{\lambda}\sqrt{\lambda^2 - 1} = \frac{R}{\lambda}\left(\omega t_1 + \sqrt{\lambda^2 - 1}\right) \tag{5}$$

$$x_2 = V_m \frac{\pi}{2\omega} = \frac{\pi R}{2\lambda} \tag{6}$$

$$\Delta x = x_1 - x_2 \tag{7}$$

where, t_1 is the time the reel vertically inserts into the crop mass (s), and t_2 is the time when the reel's action concludes (s); x_1 is the distance from the reel's center axis to the point of action when the reel is vertically inserted (mm); x_2 is the distance from the reel's center axis to the point of action when the reel's action ends (mm); and Δx represents the effective range of the reel's action (mm).

By combining Equations (5)–(7), we can derive the following equation:

$$\Delta x = \frac{R}{\lambda}\left(arcsin\frac{1}{\lambda} + \sqrt{\lambda^2 - 1} - \frac{\pi}{2}\right) \tag{8}$$

During the operation of the combine harvester, the effectiveness η of the reel is determined by the effective range Δx (mm) of the finger bar and the spacing S (mm) between the loops of the reel's cycloidal trajectory. The effectiveness η can be expressed as the following equation:

$$\eta = \frac{\Delta x}{S} \tag{9}$$

where the spacing S (mm) between the loops of the reel's cycloidal trajectory can be calculated using the following equation:

$$S = V_m \frac{2\pi}{z\omega} = \frac{2\pi R}{z\lambda} \tag{10}$$

Substituting Equations (8) and (10) into Equation (9) yields the following equation:

$$\eta = \frac{z}{2\pi} \left(arcsin\frac{1}{\lambda} + \sqrt{\lambda^2 - 1} - \frac{\pi}{2} \right) \tag{11}$$

where z is the number of axles of the reel, taken as $z= 5$ in this work.

Equation (11) was imported into MATLAB 2020 (MathWorks, Natick, MA, USA) software for curve plotting to identify the relationship between the effectiveness η of the grain separator and the speed ratio λ, as shown in Figure 11. It can be observed from Figure 11 that the effectiveness η increases continuously with the value of the speed ratio λ. For common crops such as rice and wheat, the effectiveness of the reel under normal operating conditions should be approximately 0.3 [34,35]. As the effectiveness increases, with the value of λ continuously rising, the impact of the reel on the crops is intensified, leading to greater potential grain header losses.
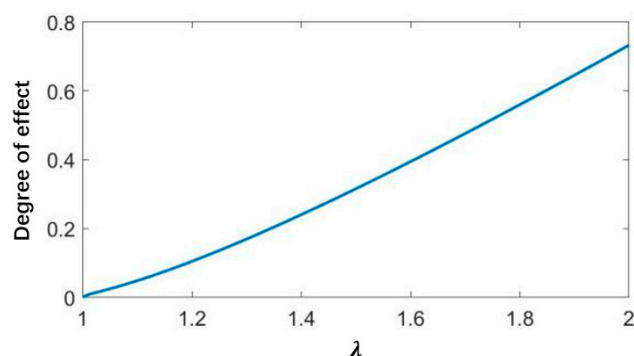
Figure 11. Function curve of reel action degree with reel speed ratio.

From Table 1, it can be concluded that the effectiveness of the grain separator remains constant at the specified speed ratio. However, when the speed ratio λ falls within the range of 1.0 to 1.5, its effectiveness is insufficient. On the other hand, when λ is between 1.6 and 2.0, the effectiveness becomes excessive, leading to excessive impact on the harvested crops and increasing losses at the header. Therefore, considering millet's susceptibility to loss upon impact when mature, a speed ratio λ between 1.5 and 1.6 is chosen for millet harvesting. In Table 1, the reason for selecting the test operating speed as 1.0 m s^{-1} is that the used combine harvester usually works in the range of $1.0–1.2 \text{ m s}^{-1}$ when harvesting to maintain the rated feed rates, and preliminary tests indicate that this combine harvester has a good harvesting performance under the operating speed; therefore, we have selected the operating speed as 1.0 m s^{-1}.

Table 1. Reel action degree under different reel speed ratio.

Operating Speed (m s^{-1})	Rotational Speed (m s^{-1})	λ Value	Working Condition	Effectiveness
1.0	0.5	0.5	Failure	/
1.0	1.0	1.0	Failure	0.003
1.0	1.5	1.5	Normal	0.27
1.0	1.6	1.6	Normal	0.36
1.0	2.0	2.0	Failure	0.61

3.3. Field Experiment Setup and Header Loss Measurement for Millet Combine Harvester

The experiment employed the 4LZ-6B millet combine harvester (Shandong Jindafeng Machinery Co., Ltd., Jining, China), setting the forward speed (V_m) of the harvester at 1.0 m s^{-1}. As shown in Figure 12, the reel speed ratio (λ) was adjusted by changing the reel's linear velocity (V_b) via the hydraulic motor. The Zhangza No. 12 millet, at the mature stage and without lodging, was selected as the experimental subject in Yantuan Town, Julu County, Hebei Province. The yield per unit area was 3104 kg hm^{-2}. Based on the statistical randomness principle, the morphological characteristics of the millet were measured, and the average plant height was determined to be 130 cm, with a moisture content of 19.4% of the crop straw.

Figure 12. 4LZ-6B Millet combine harvester. 1. Reel. 2. Hydraulic motor.

The field performance test of the millet combine harvester primarily referenced the 'Technical Specifications for Quality Evaluation of Grain Combine Harvesters'. The grain header loss was measured using the sample trough method. Based on the cutting width of the combine harvester, the sample troughs were designed with a length of 2200 mm, a width of 200 mm, and a total of three troughs. Prior to harvesting, trenches with the same dimensions as the sample troughs were dug in the test field, perpendicular to the harvester's forward direction. The trench depth was either equal to, or slightly greater than, the sample trough to prevent the trough from being crushed by the combine harvester during operation [35], as shown in Figure 13.

Figure 13. Sample trough after harvesting. 1. Stems. 2. Sampling trough. 3. Grains header loss.

After the field test of the millet combine harvester was completed, the millet heads and grains that had fallen into the sample troughs were cleaned and weighed. The grain header loss rate was then calculated according to Equation (12):

$$W = \frac{\sum_i^n W_i}{n \cdot L \cdot B_0 \cdot W_{\text{total}}} \times 100\% \tag{12}$$

where W is the cutting platform loss rate, %; W_{total} is the total millet yield in the sampled area, g; L is the length of the test area, m; B_0 is to the width of the sample trough, m; W_i is the mass of millet grains collected in the i-th sample trough, g; and n is the number of sample troughs, dimensionless.

The millet grain header loss rate was obtained based on Equation (12), as shown in Figure 14.
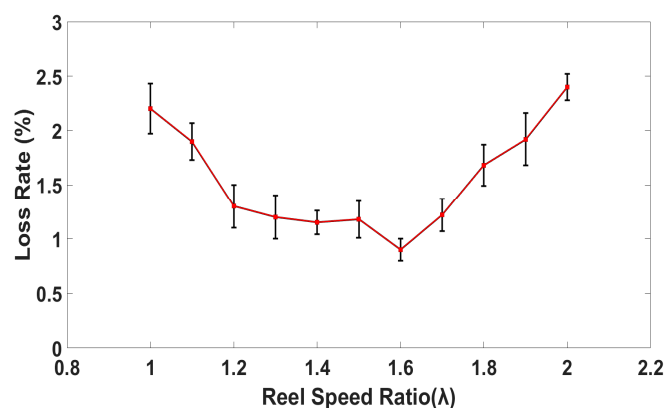
Figure 14. Variation in millet loss rate under different reel speed ratios (λ).

From Figure 14, it can be observed that, when the reel speed ratio and the height of the millet plant are fixed, the effectiveness of the reel remains constant. However, the impact of the reel varies significantly depending on the reel speed ratio (λ). Field experiments further verified the simulation results. When λ was controlled between 1.5 and 1.6, the header loss rate was the lowest. When $\lambda = 1.6$, the millet loss rate was the lowest at 0.9%. When λ is between 1.0 and 1.5, the effectiveness of the reel is insufficient. This results in a weaker force applied to the millet stalks, leading to reduced efficacy in pushing the stalks backward. Consequently, this under performance causes greater header losses. On the other hand, when λ is between 1.6 and 2.0, the reel's effectiveness becomes excessive. The force applied to the harvested crop is too strong, and at the mature stage, the connection between the millet seeds and the branches is relatively weak. As a result, excessive force can cause seeds to be dislodged, leading to further losses at the header. In contrast, when the reel speed ratio λ is between 1.5 and 1.6, the motion trajectory of the reel follows a cycloid path. Theoretical analysis shows that, at any point along this trajectory, the motion of the reel has a horizontal backward velocity. This backward motion effectively pushes the header, enabling it to cut the crop without causing excessive impact. The force exerted by the reel is moderate at this point, which prevents damage to the seed-branch connection. As a result, the millet ears remain intact on the stalk, minimizing the grain header losses. Considering the tendency for millet seeds to easily detach under impact at maturation, it is most effective to choose the optimal reel speed ratio λ between 1.5 and 1.6 during harvesting. This range ensures minimal grain header loss. These findings offer valuable insights for optimizing the adjustment of the reel mechanism in combine harvesters. By adopting this recommended range, operators can effectively reduce millet loss rates, thereby enhancing harvesting efficiency and increasing overall economic returns.

4. Conclusions

In this paper, the key dimensions of the reel of the millet harvester are determined. Based on the morphological characteristics and mechanical properties of millet plants at the mature stage, the radius of the reel was determined to be 450 mm, the installation height was 1130 mm, and the retraction distance of the reel center axis cutter was 250 mm. The three-dimensional modeling of the reel is carried out by using SolidWorks software, and the kinematics simulation analysis is introduced into RecurDyn software. It is concluded that the motion trajectory of the reel is a co-cycloid when the reel speed ratio $\lambda > 1$, which verifies the accuracy of the structural design of the reel. At the same time, this study takes the best degree of action of the reel as a prerequisite, and concludes that the reel speed ratio of the millet combine harvester header should be between 1.5 and 1.6 when harvesting millet, which provides a reference for the determination of the reel speed ratio when the combine harvester harvests millet. Through field experiments, the mature millet variety 'Zhangza No.12' was selected as the test object, and the loss rate of the header was measured under different speed ratios. The results show that the header has the lowest grain header loss rate when the reel revolution speed ratio is 1.6, which further verifies the accuracy of the simulation analysis. This study provides a theoretical basis and experimental support for the reasonable setting of the speed ratio of the reel of the millet combine harvester, which effectively reduces the grain header loss rate. The results are most directly applicable to foxtail millet under the specific conditions studied (e.g., soil type, climate, and farm size). However, we acknowledge that the performance of the combine harvester may vary with other millet species, which could have different growth patterns or harvesting requirements. Additionally, the findings in this study may be influenced by regional variations in harvesting conditions, such as moisture levels, weather patterns, and the stage of crop maturity at harvest. Testing the reel with different crop varieties and including control groups using conventional reel designs would provide valuable insights into its adaptability and overall performance. Future research could incorporate evaluations of soil impact, energy efficiency, and ecological sustainability to ensure that improvements in crop harvesting align with environmental conservation goals.

Institutional Review Board Statement: Not applicable.

Data Availability Statement: The raw data supporting the conclusions of this article will be made available by the authors on request.

Conflicts of Interest: The authors declare no conflicts of interest.

References

1. Wang, Y.; Yuan, J.; Zhong, X.; Yao, X.; Fan, G.; Liu, Y.; Zhao, Z. Research progress in nutritional function of millet. *J. North. Agric.* **2022**, *50*, 113–118.
2. Yu, Z.W.; Li, Y.M.; Du, X.X.; Liu, Y.B. Threshing cylinder unbalance detection using a signal extraction method based on parameter-adaptive variational mode decomposition. *Biosyst. Eng.* **2024**, *244*, 26–41. [CrossRef]

3. Liu, Y.B.; Li, Y.M.; Zhang, T.; Huang, M.S. Effect of concentric and non-concentric threshing gaps on damage of rice straw during threshing for combine harvester. *Biosyst. Eng.* **2022**, *219*, 1–10. [CrossRef]

4. Wang, F.Z.; Liu, Y.B.; Ji, K.Z. Research and experiment on variable-diameter threshing drum with movable radial plates for combine harvester. *Agriculture* **2023**, *13*, 1487. [CrossRef]

5. Ma, Z.; Zhang, Z.L.; Zhang, Z.H.; Song, Z.Q.; Liu, Y.B.; Li, Y.M.; Xu, L.Z. Durable testing and analysis of a cleaning sieve based on vibration and strain signals. *Agriculture* **2023**, *13*, 2232. [CrossRef]

6. Zhang, T.; Li, Y.M.; You, G.L. Experimental study on the cleaning performance of hot air flow cleaning device. *Agriculture* **2023**, *13*, 1828. [CrossRef]

7. Chen, S.; Zhou, Y.; Tang, Z.; Lu, S. Modal vibration response of rice combine harvester frame under multi-source excitation. *Biosyst. Eng.* **2020**, *194*, 177–195. [CrossRef]

8. Qing, Y.R.; Li, Y.M.; Xu, L.Z.; Ma, Z.; Tan, X.L.; Wang, Z. Oilseed rape (*Brassica napus* L.) pod shatter resistance and its relationship with whole plant and pod characteristics. *Ind. Crops Prod.* **2021**, *166*, e113459.

9. Hobson, R.; Bruce, D. PM—power and machinery: Seed loss when cutting a standing crop of oilseed rape with two types of combine harvester header. *Biosyst. Eng.* **2002**, *81*, 281–286. [CrossRef]

10. Hirai, Y.; Inoue, E.; Mori, K.; Hashiguchi, K. PM—Power and machinery investigation of mechanical interaction between a combine harvester reel and crop stalks. *Biosyst. Eng.* **2002**, *83*, 307–317. [CrossRef]

11. Wu, W.; Wu, C. Optimization for header parameters of rape combine harvester. *J. Zhejiang Univ. (Agric. Life Sci.)* **2018**, *44*, 481–489.

12. Xue, Z.; Fu, J.; Fu, Q.; Li, X.; Chen, Z. Modeling and optimizing the performance of green forage maize harvester header using a combined response surface methodology-artificial neural network approach. *Agriculture* **2023**, *13*, 1890. [CrossRef]

13. Zhao, J. Design and Test of 4LZG-1.5 small self-propelled millet harvester. *Agric. Eng.* **2022**, *12*, 109–112. [CrossRef]

14. Zheng, G.; Li, Y.; Ji, K.; Liang, Z.; Ma, X.; Cheng, J. Vibration analysis and structural optimization of header frame of millet combine harvester. *Agric. Mech. Res.* **2024**, *46*, 41–45+53. [CrossRef]

15. Yang, S.; Yang, S.; She, Y. Computer simulation of the motion trajectory of the reel. *J. Agric. Mech. Res.* **2010**, *32*, 141–145. [CrossRef]

16. Li, Y.M.; Li, Y.W.; Xu, L.Z.; Hu, B.Y.; Wang, R. Structural parameter optimization of combine harvester cutting bench. *Trans. Chin. Soc. Agric. Eng.* **2014**, *30*, 30–37.

17. Ji, K.; Li, Y.; Liang, Z.; Liu, Y.; Cheng, J.; Wang, H.; Zhu, R.; Xia, S.; Zheng, G. Device and method suitable for matching and adjusting reel speed and forward speed of multi-crop harvesting. *Agriculture* **2022**, *12*, 213. [CrossRef]

18. Li, C. Design and Experimental Study on Low-Loss Header of Millet Combine Harvester. Master's Thesis, Henan University of Science and Technology, Luoyang, China, 2019.

19. Du, J.; Jiang, B.; Yin, H.; Zhang, L.; Jin, C.; Yin, X. Development of automatic control system for the rotation speed of combine harvester reel. *J. Chin. Agric. Mech.* **2020**, *41*, 1–5. [CrossRef]

20. Jiangsu Institute of Technology. *Agricultural Machinery Science*; China Agricultural Machinery Press: Beijing, China, 1978.

21. Du, X.; Ji, J.; Jin, X.; Li, C.; Yang, X. Research on divider losses with high-speed photography for foxtail millet harvesting. *Future Gener. Comput. Syst.* **2018**, *88*, 55–60. [CrossRef]

22. Liang, Z.W.; Eyasu, W.M. Development of cleaning systems for combine harvesters: A review. *Biosyst. Eng.* **2023**, *236*, 79–102. [CrossRef]

23. Chen, M.; Jin, C.; Ni, Y.; Yang, T.; Zhang, G. Online field performance evaluation system of a grain combine harvester. *Comput. Electron. Agric.* **2022**, *198*, 107047. [CrossRef]

24. Li, B.F. *Agricultural Mechanics*; China Agriculture Press: Beijing, China, 2003.

25. Qing, Y.; Li, Y.; Yang, Y.; Xu, L.; Ma, Z. Development and experiments on reel with improved tine trajectory for harvesting oilseed rape. *Biosyst. Eng.* **2021**, *206*, 19–31. [CrossRef]

26. Wang, J.; Wang, Z.; Jia, J.; Ye, H. Guide rail trajectory of mower table reel device for silage harvester. *Trans. Chin. Soc. Agric. Mach.* **2011**, *42*, 152–155.

27. Yang, R.; Wang, Z.; Shang, S.; Zhang, J.; Qing, Y.; Zha, X. The design and experimentation of EVPIVS-PID harvesters' header height control system based on sensor ground profiling monitoring. *Agriculture* **2022**, *12*, 282. [CrossRef]

28. Zareei, S.; Abdollahpour, S. Modeling the optimal factors affecting combine harvester header losses. *Agric. Eng. Int. CIGR J.* **2016**, *18*, 60–65.

29. Hu, Z.D.; Du, S.R.; Yang, J.B. Simulation study on the combined harvester with four tracked feet passing through ditch based on RecurDyn. *Appl. Mech. Mater.* **2014**, *3072*, 756–762. [CrossRef]

30. Xiang, J.; Yang, L.; Li, S. Structural design of the base cutter for mini-type sugarcane harvester. *Trans. Chin. Soc. Agric. Mach.* **2008**, *39*, 56–59.

31. He, J.; Tong, J.; Chen, Z.; Fang, X.; Han, Z. Virtual design and kinematic simulation for feed-in mechanism with finger rotor. *Trans. Chin. Soc. Agric. Mach.* **2007**, *38*, 53–56.

32. Yang, Y.; Li, Y.; Qing, Y. Analysis and experiment on the feeding trajectory of the reel for rapeseed combine harvester. *J. Agric. Mech. Res.* **2020**, *42*, 189–194. [CrossRef]

33. Dong, Y. Simulation of the Motion Orbit and Experimental Study of the Reel for Rape Combine Harvester Header. Master's Thesis, Jiangsu University, Zhenjiang, China, 2008.

34. Zhang, M.; Li, G.; Yang, Y.; Jin, M.; Jiang, T. Design and parameter optimization of variable speed reel for oilseed rape combine harvester. *Agriculture* **2023**, *13*, 1521. [CrossRef]

35. Lan, X.; Li, M. A new method for determining loss rate of rapeseed harvester header: Sample slot measurement method. *J. Agric. Mach. Qual. Superv.* **2012**, *8*, 19–21.